Domain Reorientation and Induced Fit upon RNA Binding: Solution Structure and Dynamics of Ribosomal Protein L11 from *Thermotoga maritima*

Sergey Ilin,[a, b] Aaron Hoskins,[b] Oliver Ohlenschläger,[c] Hendrik R. A. Jonker,[a] Harald Schwalbe,*[a] and Jens Wöhnert*[a]

L11, a protein of the large ribosomal subunit, binds to a highly conserved domain of 23S rRNA and mediates ribosomal GTPase activity. Its C-terminal domain is the main determinant for rRNA binding, whereas its N-terminal domain plays only a limited role in RNA binding. The N-terminal domain is thought to be involved in interactions with elongation and release factors as well as with the antibiotics thiostrepton and micrococcin. This report presents the NMR solution structure of the full-length L11 protein from the thermophilic eubacterium Thermotoga maritima *in its free form. The structure is based on a large number of orientational restraints derived from residual dipolar couplings in addition to conventional NOE-based restraints. The solution structure of L11 demonstrates that, in contrast to many other multidomain RNA-binding proteins, the relative orientation of the two domains is well defined. This is shown both by heteronuclear ^{15}N-relaxation and residual dipolar-coupling data. Comparison of this NMR structure with the X-ray structure of RNA-bound L11, reveals that binding not only induces a rigidification of a flexible loop in the C-terminal domain, but also a sizeable reorientation of the N-terminal domain. The domain orientation in free L11 shows limited similarity to that of ribosome-bound L11 in complex with elongation factor, EF-G.*

Introduction

The formation of RNA–protein complexes is often accompanied by major conformational changes in both the RNA and protein components. This has been described as a "mutually induced fit" or adaptive binding.[1] In many cases, dynamically disordered parts of either one of the binding partners adopt a defined conformation in the complex. Furthermore, for many multidomain RNA-binding proteins, it has been found that the relative orientation of the domains is not defined in the RNA-free form but is well defined in the RNA–protein complex.[2–5] These conformational adaptations, which occur on different structural levels, are thought to be important for affinity and specificity in RNA–protein interactions. Consequently, a complete picture of RNA–protein recognition processes often emerges only once the structures of the components are known in their free and bound conformations.

The ribosomal protein L11 is a highly conserved two-domain protein that binds to a conserved 58-nucleotide sequence in the 23S rRNA of the large ribosomal subunit. The complex between L11 and its cognate 23S-rRNA domain is an essential part of the ribosomal GTPase-associated region and is involved in the GTPase activity of the elongation factors EF-G and EF-Tu.[6,7] Reconstituted ribosomes that lack native L11 protein show a twofold slower rate of de novo protein synthesis than normal ones. Also, they are defective, for example, in EF-G-dependent GTP hydrolysis and release factor 1 (RF-1) dependent termination.[8,9]

The L11–RNA complex is a target of the thiazole family of antibiotics that includes thiostrepton and micrococcin.[10–12] These antibiotics inhibit ribosome function by interfering with the interaction of EF-G and EF-Tu–aminoacyl–tRNA–GTP (EF-Tu–aa–tRNA–GTP) complex with the large 50S ribosomal subunit. The affinity of thiostrepton for the 23S rRNA domain is greatly increased in the presence of full-length L11 but not with the C-terminal domain alone.[13]

The structures of full-length L11 from *Thermotoga maritima* and the C-terminal domain of L11 from *Bacillus stearothermophilus* bound to their cognate RNA have been solved by X-ray crystallography.[14,15] In addition, the conformation of the C-terminal domain of L11 from *B. stearothermophilus* has been characterized in its RNA-bound and free forms by NMR.[16–18] Nota-

[a] *S. Ilin, Dr. H. R. A. Jonker, Prof. Dr. H. Schwalbe, Dr. J. Wöhnert*
Institute of Organic Chemistry and Chemical Biology
Center for Biomolecular Magnetic Resonance
Johann Wolfgang Goethe Universität
Marie-Curie-Straße 11, 60439 Frankfurt am Main (Germany)
Fax: (+49) 69-798-29515
E-mail: schwalbe@nmr.uni-frankfurt.de
jewoe@nmr.uni-frankfurt.de

[b] *S. Ilin, A. Hoskins*
Department of Chemistry, Massachusetts Institute of Technology
77 Massachusetts Avenue, Cambridge, MA 02139 (USA)

[c] *Dr. O. Ohlenschläger*
Institut für Molekulare Biotechnologie (IMB)
Abteilung Molekulare Biophysik/NMR Spektroskopie
Beutenbergstraße 11, PF 100 813, 07708 Jena (Germany)

Supporting information for this article is available on the WWW under http://www.chembiochem.org or from the author.

 DOI: 10.1002/cbic.200500091

bly, the X-ray structure of the complex from *T. maritima* has indicated possible conformational dynamics for the L11 protein.[14] Whereas the C-terminal domain was tightly packed against the RNA, as was expected from biochemical studies,[13] the N-terminal domain showed only limited RNA–protein interactions. In addition, weak electron density and high B-factors for the entire domain indicated rigid body motion of the N-terminal domain in the crystal.[14] Furthermore, in the X-ray structure of the large ribosomal subunit from *Deinococcus radiodurans*,[19] a domain orientation different from that in the isolated complex was found. However, in the crystal structure of the large ribosomal subunit from *Haloarcula marismortui*, the L11 region is completely disordered.[20] This indicates that this region undergoes dynamic conformational changes.

Remarkably, cryoelectron microscopy (cryo-EM) and biochemical studies of the ribosome indicate an important functional role for the conformational dynamics of L11 during the ribosomal cycle. The binding of the EF-Tu–aa–tRNA–GTP complex leads to a large scale conformational rearrangement of the GTPase-associated center of the ribosome and results in direct contact between the rRNA and the elbow region of the aa–tRNA.[21] In addition, Frank and co-workers showed that the position of the N-terminal domain of L11 shifted upon binding of EF-G–GTP to the ribosome and shifted even further after GTP hydrolysis.[22] In line with these findings, thiostrepton is thought to inhibit the translocation step of the elongation cycle by blocking conformational rearrangement of the L11 N-terminal domain. This in turn blocks conformational rearrangement of the EF-G–ribosome complex after GTP-hydrolysis.[23,24] In addition, in vivo genetic experiments have demonstrated that it is the N-terminal domain of L11 that is important for mediating the interaction of the ribosome with RF-1 and its function in UAG-mediated termination,[25] which can again be blocked by thiostrepton.[26]

To obtain a more detailed picture of the dynamic processes that accompany RNA–protein interaction in the L11–RNA complex, we investigated the conformation and dynamics of the full-length L11 (amino acids 1–141). The protein from the hyperthermophilic eubacterium *T. maritima* was investigated in its free form in solution by using NMR spectroscopy. In particular, the relative orientation of the N- (amino acids 1–71) and C-terminal (amino acids 75–141) domains of the protein in its free form were investigated by the analysis of long-range structural information derived from heteronuclear-relaxation rates and residual dipolar couplings. We show that the relative orientation of the two domains is rigid and well defined in solution. Comparison of the solution structure of the free protein with the RNA-bound conformation, however, indicates a domain reorientation upon RNA binding.

Results

Assignment

As reported previously,[27] essentially complete backbone assignments could be obtained with the exception of Met1, Ala2, Pro22, and Pro73, the latter two preceding proline residues. Side-chain assignments are complete except for the Pro74–Phe78 region (Figure 1).

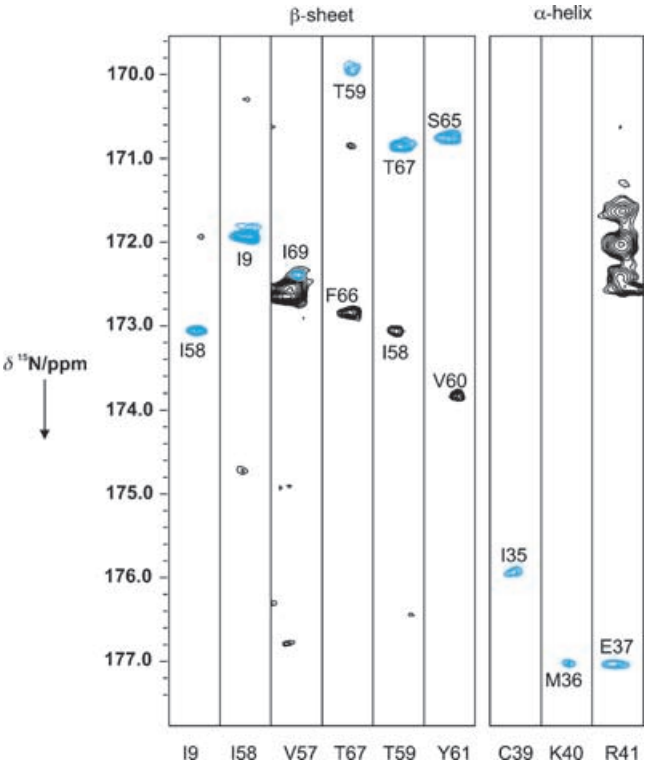

Figure 1. Strips taken from a 3D HNCO experiment that was optimized for the detection of through-hydrogen-bond $^{2h}J(N,C')$ scalar couplings. The results are for residues in the central β-sheet and α-helix α3 of the N-terminal domain of L11. Cross peaks (blue) correspond to $^{2h}J(N,C')$ couplings that are due to the presence of a hydrogen bond. Black contours are due to through-bond $^{1}J(N,C')$ couplings that were not completely suppressed by the pulse sequence.

Structure determination

The tertiary structure of L11 was determined by using the torsion-angle simulated annealing protocol as implemented in the CNX 2002 program. A total of 4276 restraints (Table 1), which represent an average of ~30 nontrivial restraints per residue for amino acids 3–141, were used as the input for structure calculations. These included 3584 NOE-based restraints, 179 torsion-angle restraints, 84 hydrogen-bond restraints, and 429 restraints derived from residual dipolar couplings. The 20 structures with the lowest overall energy and least NOE violations were chosen from an ensemble of 50-calculated structures to represent the solution structure of L11. These 20 structures were subjected to an additional round of restrained energy minimization. However, residual dipolar-coupling restraints in the relaxation-matrix refinement of the prefolded structures were excluded.[28]

The structural statistics are given in Table 2. The superimposed backbone coordinates of the 20 lowest energy structures are well aligned for the N-terminal domain (residues 5–72). They have root-mean-square-deviation (RMSD) values of 0.28 Å (0.77 Å) for all backbone (heavy) atoms. The RMSD value

Table 1. Experimental restraints.

Distance restraints	
intraresidue ($i-j=0$)	970
sequential ($\|i-j\|=1$)	989
medium-range ($\|i-j\|=5$)	698
long-range ($\|i-j\|>5$)	917
interdomain	10
hydrogen bonds	84
total	3668
distance restraints/residue[a]	26.4
Dihedral-angle restraints	
φ, ψ(TALOS)	77
J-coupling restraints:	
HNHA	102
RDC restraints:	
N–H	92
C^{α}–H^{α}	72
H^{N}–C'	91
N–C'	90
C^{α}–C'	84
total	429
restraints/residue[a]	30.7

[a] Amino acids 3–141.

Table 2. Characterization of the ensemble of 20 NMR structures obtained from *T. maritima* L11.

CNX energies [kcal mol^{-1}][a]	
E_{total}	576.51 ± 55.46
E_{bond}	40.82 ± 6.42
E_{angle}	184.74 ± 19.13
$E_{improper}$	29.73 ± 13.99
E_{vdw}	53.62 ± 6.73
E_{NOE}	208.47 ± 39.24
E_{cdih}	8.64 ± 3.32
RMSD of the 20 best structures	
NTD backbone atoms [Å]	0.28
NTD heavy atoms [Å]	0.77
CTD backbone atoms [Å]	0.36
CTD heavy atoms [Å]	1.24
all backbone atoms [Å]	0.69
all heavy atoms [Å]	1.70
RMSD from idealized geometry	
bonds [Å]	0.0046 ± 0.0004
angles [°]	0.6843 ± 0.0402
impropers [°]	0.6484 ± 0.0590
RMSD from experimental restraints[b]	
distances [Å]	0.0389 ± 0.0036
dihedral angles [°]	14.4188 ± 0.7925
$^{3}J_{HNHA}$ coupling [Hz]	2.4896 ± 0.1187
Ramachandran analysis of N-terminal domain [%][c]	
residues in most-favored regions	59.6
residues in additional allowed regions	30.8
residues in generously allowed regions	9.6
residues in disallowed regions	0
Ramachandran analysis for region 75–141 [%][c]	
residues in most-favored regions	83.7
residues in additional allowed regions	14.3
residues in generously allowed regions	0.0
residues in disallowed regions	2.0

[a] These values were estimated by using CNX 2002. The final values of the force constants used for the calculations are as follows: 1000 kcal mol^{-1} Å^{-2} for bond lengths; 500 kcal mol^{-1} rad^{-2} for bond angles and improper torsions; 4 kcal mol^{-1} Å^{-4} for the van der Waals term; 50 kcal mol^{-1} Å^{-2} for NOE-derived and hydrogen-bonding distance restraints; 200 kcal mol^{-1} rad^{-2} for dihedral angle restraints; and 0.8 kcal mol^{-1} Hz^{-2} for residual dipolar coupling restraints. [b] The distance restraints include NOEs as well as hydrogen-bonding restraints. [c] The values were calculated for residues 8–72, 75–86, and 96–141 by using PROCHECK.[51]

for the C-terminal domain (residues 75–141) is 0.36 Å (1.24 Å) for all backbone (heavy) atoms due to the presence of a dynamically disordered loop that spans residues 84–96. When only the well-ordered regions of the C-terminal domain were considered (residues 75–82, 96–141) the RMSD was 0.29 Å (0.82 Å).

Structure of the domains

The N-terminal domain exhibits a compact fold that consists of a three-stranded antiparallel β-sheet and two α-helices (Figure 2A, left). The four N-terminal residues are structurally disordered. The connectivity of the secondary-structure elements is β1–α1–α2–β2–β3. The two α-helices are packed against the surface of the β-sheet. The N-terminus of helix α1 is formed by two consecutive proline residues, Pro22 and Pro23. Interestingly, the ^{13}C-chemical shift difference between C_{γ} and C_{β} of Pro23 indicates that the peptide bond preceding Pro23 is in the *cis* conformation.[29] All other peptide bonds preceding proline residues are in the *trans* conformation. The C-terminal domain consists of a short two-stranded parallel β-sheet and three α-helices (Figure 2A, right). The connectivity of the secondary structure elements is α3–β4–α4–α5–β5. The structure of the loop connecting α3 and β4 (residues 84–96) is not defined by the NMR data. The backbone amide groups of this loop exchange rapidly with D_2O and exhibit reduced ^{1}H{^{15}N}-HetNOE values; this indicates dynamic disorder in this region (Figure 3).

The individual structures of the two domains of free L11 are very similar to those in the RNA-bound state.[14] The average RMSD value between the family of NMR and X-ray structures for the N-terminal domain (residues 8–72) is 1.11 ± 0.05 Å. The average RMSD value between the family of NMR and X-ray structures for the C-terminal domain (residues 75–141) is 2.34 ± 0.63 Å. The larger RMSD value for the C-terminal domain is due to differences in the structure of the loop that connects helix α3 and strand β4 (residues 84–96, β-loop), which is disordered in the NMR-structure, and of the loop that connects helices α5 and α6. When considering only residues in stable secondary-structure elements, the RMSD for the C-terminal domain in its free and bound forms drops to 0.97 ± 0.07 Å. Both of these disordered loops in the C-terminal domain are involved in protein–RNA interactions and undergo an "induced-fit" conformational change upon RNA-binding.[14,16] However, beside residues with disordered side-chain and backbone conformation in the free state of the protein, the RNA-

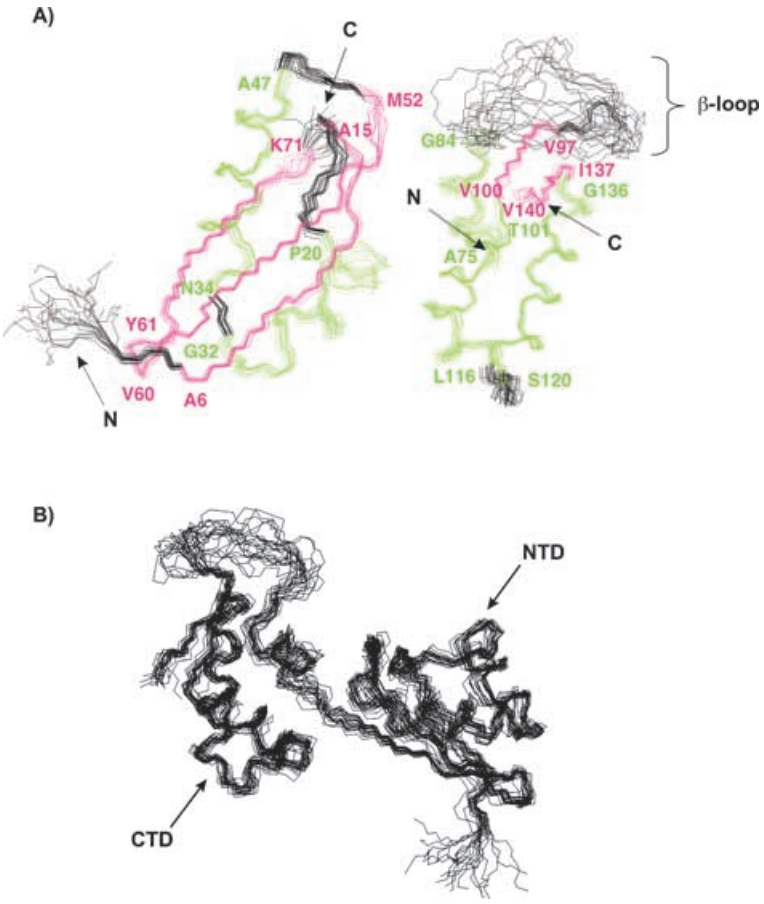

Figure 2. NMR solution structure of L11 from *T. maritima* in its free form. The 20 NMR solution structures with the lowest energy were superimposed after energy minimization. All backbone heavy atoms were used for the least-square superposition. A) Separate superposition of the isolated N- (amino acids 1–72, left) and C-terminal (amino acids 75–142, right) domains (NTD and CTD, respectively). α-helices are indicated in green and β-strands in red. The boundaries of the secondary-structure elements are indicated. The dynamically disordered loop that connects amino acids 84–96 (β-loop) in the C-terminal domain is marked. B) Superposition of the structural ensemble that was obtained for the full-length protein by using the orientational information that is inherent in the residual dipolar-coupling data.

binding surface of the C-terminal domain contains a significant number of amino acids with side-chain conformations that are very similar to those in the RNA-bound form (Figure 3).[14] These amino acids are mainly located in helices α3 and α6. Thus, the RNA-binding surface of the CTD is a partially preordered RNA recognition platform.

Relative orientation of the domains

The two domains are connected by a short three-amino-acid linker that is conformationally highly restricted since it contains two consecutive proline residues (Thr72–Pro73–Pro74).

Figure 4 shows the longitudinal and transversal ^{15}N-relaxation rates, R_1 and R_2. Uniform R_1 and R_2 values are observed for most amino acids in both the N- and C-terminal domains of the protein. Residues in the disordered β-loop of the C-terminal domain (see above) are the only notable exceptions. The ratio R_2/R_1 was used to calculate the overall rotational-correlation times τ_C for the N- and C-terminal domains and for the entire protein by using the Tensor 2.0 program.[30] Only residues in stable secondary structures with a ^{1}H{^{15}N}-HetNOE > 0.8 were taken into account. The overall rotational-correlation times for the N- and C-terminal domains were 9.04 and 9.49 ns, respectively; it was found to be 9.20 ns for the full-length L11 protein. Based on the Stokes–Einstein equation, these values should be expected for an extended protein that has an axially symmetric rotational-diffusion tensor $(D_\parallel/D_\perp) = 1.78$, as calculated from the solution structure of the free L11 and a molecular weight of ~15 kDa. This correlates well with the molecular weight of the full-length L11 protein. In contrast, an overall rotational-correlation time of 6.0 and 5.8 ns for the N- and C-terminal domains, respectively, would be expected if the two domains tumbled completely independently in solution. Thus, the close agreement of the rotational-correlation time of the separate domains with the τ_c of the whole protein, and the value predicted based on the Stokes–Einstein equation indicate that L11 tumbles as a single rigid unit in solution and the relative orientation of the domains is well defined. In addition, none of the backbone amides close to or in the linker region show signs of increased internal dynamics. The ^{1}H{^{15}N}-HetNOEs, R_1-, and R_2-relaxation rates that could be measured in the region between amino acids 65–80, are all very similar to the values found for the remainder of the protein (Figure 4).

However, only a limited number of interdomain NOEs could be reliably assigned between the N- and C-terminal domains of L11. These include NOEs between the side chains of residues Met52, Leu54, and Thr72 of the N-terminal domain and Leu78, Thr111, Pro114, and Leu116 of the C-terminal domain. By using this limited amount of NOE-information, the relative orientation of the two domains was not defined unambiguously in the initial set of structure calculations. However, incorporation of orientation information that was provided by a large number of ^1D(N,H), ^1D(N,C′), ^2D(H$_N$,C′), and ^1D(C′,C$_\alpha$) residual dipolar couplings into the calculations, allowed the determination of the relative domain orientation (Figure 2B).

Comparison of domain orientation of free and RNA-bound L11

To compare the domain orientation of L11 free in solution with that in the RNA-bound form,[14] we aligned the C-terminal domains of L11 in the two structures. Figure 5 shows all backbone heavy atoms (residues 75–141, excluding residues 84–96) in the disordered β-loop. In the structure of the free form of L11, the N-terminal domain is moved away from the RNA surface so that a cleft is opened between the protein and the RNA. Helix α1, as well as the RNA hairpin loop that contains residues A1067 and A1095, become more exposed to the sol-

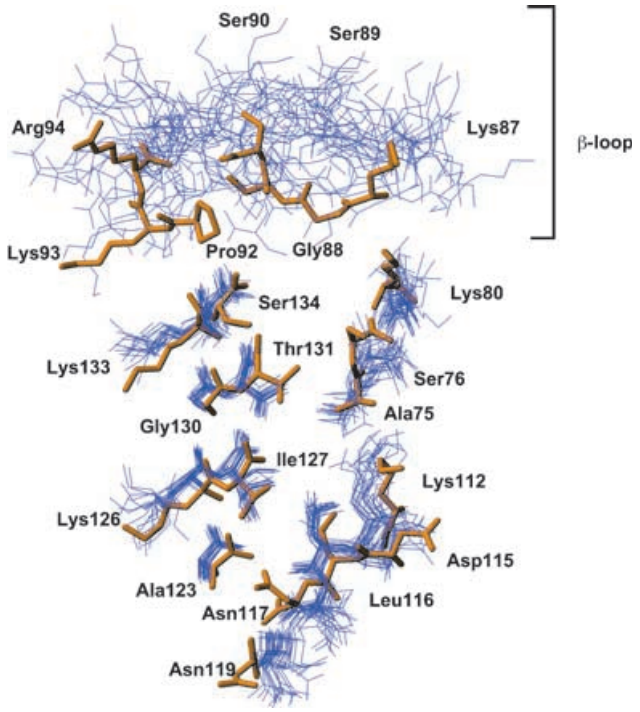

Figure 3. The RNA-binding surface of the C-terminal domain is a partially preorganized RNA recognition platform. The side-chain conformations of amino acids that are involved in RNA-binding obtained from the RNA–L11 X-ray structure[14] (gold) are compared with those from the NMR solution structure of free L11 (blue).

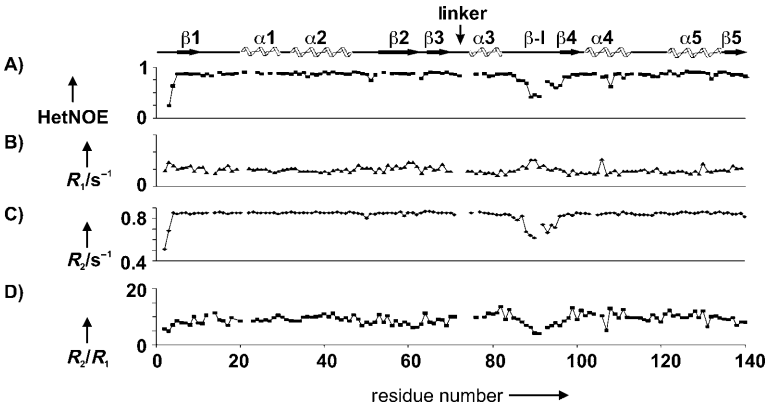

Figure 4. Internal dynamics of L11 free in solution. A) Backbone amide $^{1}H\{^{15}N\}$-HetNOE values, B) backbone ^{15}N R_1-relaxation rates, C) backbone ^{15}N R_2-relaxation rates, and D) the R_2/R_1 ratios for *T. maritima* L11 at 25 °C. The data were recorded at a field strength of 14.1 T. The positions of the stable secondary-structure elements along the sequence are indicated and the location of the dynamically disordered β-loop is highlighted. The interdomain linker is located between strand β3 and helix α3.

vent. Thus, no RNA–protein interactions would be possible for the N-terminal domain in the free conformation.

Furthermore, we compared the structure of free L11 with that bound to the 70S ribosome (pdb 1JQT), 70S ribosome–EF-G–GTP (pdb 1JQS), EF-G–GDP–fusidic acid (pdb 1JQM),[22] 70S ribosome–recycling factor (RF-2; pdb 1ML5),[31] 70S ribosome– EF-Tu–GDP–Kirromycin (pdb 1R2X) complexes,[21] and also to the structure of the *D. radiodurans* L11 bound to the

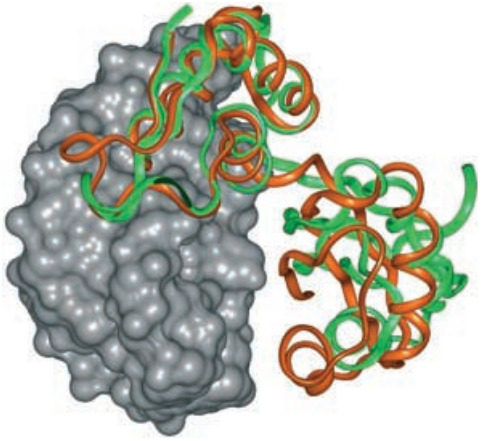

Figure 5. Relative orientation of the N-terminal domain of L11 to L11-bound RNA[14] and free L11. To compare the relative domain orientation in the two structures, only the two C-terminal domains are superimposed. The RNA is depicted as a van der Waals surface representation in gray, the backbone trace of bound L11 is shown in red and free L11 in green.

50S ribosomal subunit (pdb 1NKW).[19] The domain orientation of free L11 is different to its conformation in all these ribosomal complexes. The closest resemblances in the domain orientation are found when comparing our structure to the L11 structures in the EF-G–GTP and EF-G–GDP–ribosomal complexes (Figure 6B and C). In fact, the domain orientation of the free L11 seems to be an intermediate between that found in these two complexes (Figure 6B and C). To obtain a more quantitative measure for the similarity of the domain orientation in the different complexes, we aligned the equivalent C_α positions of the C-terminal domain of L11 free in solution with that in the complexes. We then calculated the pairwise RMSD of the equivalent C_α positions of the unaligned N-terminal domains. The results are given in Table 3. RMSD values of 5.76 and 6.05 Å were obtained for the difference in N-terminal domain C_α positions between free and ribosome-bound L11 in complex with EF-G–GDP and EF-G–GTP, respectively. The largest deviation was found for the orientation of the N-terminal domain of free L11 and the EF-Tu complex (12.71 Å).

Discussion

A common theme for the description of the interaction of RNA with multidomain RNA-binding proteins is the notion that the domain orientation in the free protein is flexible and becomes well defined only upon RNA binding. Here, we present the solution structure of the ribosomal protein, L11, from the hyperthermophilic bacterium *T. maritima* in its free form. L11 is a two-domain RNA-binding protein. The two domains are connected only by a short linker of three amino acids that contains two proline residues. Numerous structural studies of the large ribosomal subunit in different functional states[19,21,22,31] and the isolated L11–RNA complex[14] have been carried out by using X-ray or cryo-EM

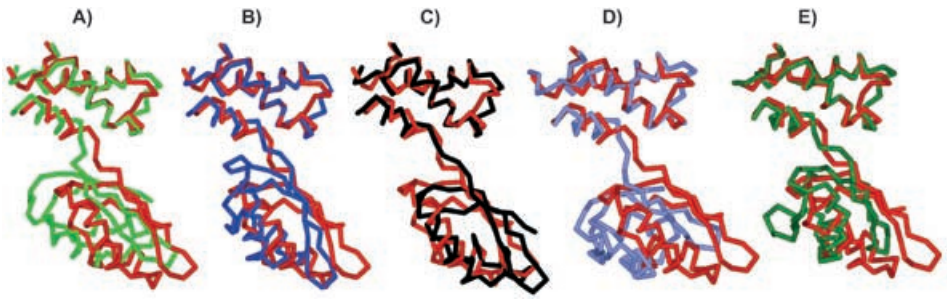

Figure 6. Comparison of the relative domain orientation of free and ribosome-bound L11 in different functional ribosomal complexes. The C-terminal domain of free L11 (red) was aligned with the C-terminal domain of: A) L11 bound to the *E. coli* 70S ribosome (green, pdb 1JQT),[22] B) L11 bound to the *E. coli* 70S ribosome–EF-G–GMPPCP complex (dark blue, pdb 1JQM),[22] C) L11 bound to the *E. coli* 70S ribosome–EF-G–GDP–fusidic acid complex (black, pdb 1JQS),[22] D) L11 bound to the *E. coli* 70S ribosome–EF-Tu–GDP–kirromycin complex (blue, pdb 1R2X),[21] and E) L11 bound to the *E. coli* 70S ribosome–RF-2 complex (dark green, pdb 1ML5).[31] The disordered β-loop region was not taken into account for the alignments and was removed for clarity.

Table 3. Comparison of the relative domain orientation of free L11 with RNA-bound L11[14] and ribosome-bound L11 in different functional complexes.[19,21,22,31] Pairwise RMSDs between free and bound L11 in equivalent C_α positions in the N-terminal domains are given. The values were obtained after the alignment of the C-terminal domains. Only C_α atoms in stable secondary-structure elements were taken into account.

	1MMS[a]	1NKW[b]	1JQT[c]	1JQS[d]	1JQM[e]	1R2X[f]	1ML5[g]
RMSD	3.95	4.86	3.87	3.42	2.75	5.75	3.94

[a] X-ray structure of *T. maritima* L11 bound to RNA;[15] [b] L11 bound to the 50S ribosomal subunit of *D. radiodurans*;[19] [c] L11 bound to the *E. coli* 70S ribosomal subunit;[22] [d] L11 bound to the *E. coli* 70S ribosomal subunit when in complex with EF-G–GTP;[22] [e] L11 bound to the *E. coli* 70S ribosomal subunit when in complex with EF-G–GDP–fusidic acid;[22] [f] L11 bound to the *E. coli* 70S ribosomal subunit when in complex with EF-Tu–GDP–kirromycin.[21] [g] L11 bound to the *E. coli* 70S ribosomal subunit when in complex with RF-2.[31]

techniques. These have revealed a number of different L11 conformations that, in concert with biochemical[13,23] and NMR data, indicate that L11 is a flexible protein with a fixed domain orientation only in its RNA-bound state. Interestingly, our NMR structure of free L11, which is based on a large number of long-range orientational restraints together with ^{15}N-relaxation data, suggests that the domain orientation of L11 is well defined even free in solution. Therefore, RNA binding to the protein does not induce a disorder-to-order transition but rather a domain-reorientation process; free L11 has a fixed domain orientation that changes upon complex formation with RNA. This domain reorientation is accompanied by an "induced-fit"-type interaction of a disordered loop in the C-terminal domain of L11. This loop becomes structured upon RNA-binding as observed by NMR spectroscopy of the isolated C-terminal domain of the *B. stearothermophilus* L11.[16–18]

A domain-reorientation process is energetically less costly for the RNA-binding process; it might lower the entropic penalty for complex formation that is associated with the transition from a disordered state to an ordered domain orientation. Therefore, it is tempting to speculate that a fixed-domain orientation in the "free" state of the protein is a mechanism for hyperthermophilic organisms to enhance the stability of RNA–protein complexes by lowering the entropic costs. Dynamic NMR studies of the C-terminal domain of L11 from the moderately thermophilic *B. stearothermophilus* (BstL11-CTD) have been carried out.[16,17] These show that BstL11-CTD in its free form is conformationally heterogeneous with respect to the *cis*–*trans* isomerization of proline peptide bonds but homogeneous in its RNA-bound form.[16] No such conformational heterogeneity is observed for free L11 from *T. maritima*. This indicates that L11 from *T. maritima* is indeed a more preordered RNA-binding platform than BstL11-CTD that favors complex formation. However, the linker length and sequence are highly conserved in L11 proteins from both mesophilic and thermophilic organisms. This linker is only three amino-acids long and includes the two prolines that contribute to restricting its conformational variability. Thus, a more or less fixed domain orientation might also be found in other L11 proteins, but no structural data are available for proteins isolated from mesophilic organisms.

It is interesting to note that the domain orientation of L11 in solution is different to all its conformations found in functional ribosomal complexes. Thus, in all these complexes, L11 must be somewhat strained compared to its ground-state conformation in solution. Taken together with the highly conserved conformational restriction of the linker itself, this suggests that L11 might act as a "spring-load" during the ribosomal cycle; that is, it stores and forwards energy by adjusting its domain orientation. This would extend the proposals that suggests a functional role for L11 conformational transitions during ribosome function.[23,24] It could also suggest that thiostrepton acts by fixing this spring in position.

Experimental Section

Sample preparation: The gene coding for L11 was cloned from *T. maritima* genomic DNA (American Type Culture Collection, 43589D) by using PCR. It was inserted into plasmid pET11a (Novagen) and over-expressed in *E. coli* BL21(DE3) either in ^{15}N- or ^{15}N/^{13}C-labeled form. This was done by growing the bacteria in M9-minimal medium that contained only ^{15}N-labeled NH_4Cl and ^{13}C-labeled glucose (Cambridge Isotope Laboratories, Cambridge, MA, USA) as the sole nitrogen and carbon sources. Purification of the protein consisted of a heat denaturation step followed by cation exchange chromatography on a SP-Sepharose column (Pharmacia). This resulted in $>95\%$ pure protein with excellent solubility and long-term stability. Samples for NMR spectroscopy contained protein (~1.2 mM) in buffer (20 mM $KHPO_4$, pH 6.2, 50 mM KCl, 10% ^2H_2O).

NMR spectroscopy: Spectra were acquired at 25 °C on Bruker DRX600 and DRX700, and Varian ^{UNITY}INOVA 600 and 750 spectrometers that were equipped with *z*-axis gradient $^1H\{^{13}C,^{15}N\}$ triple-resonance probes. Spectra were processed with XWINNMR 3.0 (Bruker) or VNMR (Varian) and analyzed with XEASY.[32]

Sequential backbone and side-chain resonance assignments were obtained from a combination of 3D HNCACB, CBCA(CO)NH, HNCO, H(CCCO)NH, (H)CC(CO)NH, HBHA(CO)NH, and HCCH-TOCSY experiments (reviewed in ref. [33]) as described elsewhere.[27] ^1H chemical shifts were referenced to TMSP at 0.00 ppm and ^{13}C and ^{15}N chemical shifts were calculated from the ^1H frequency.[34]

Distance restraints were derived from the 3D ^{15}N-edited NOESY (140 ms), 3D ^{13}C-edited NOESY (140 ms), and a 3D ^{13}C-edited NOESY (140 ms) that were optimized for the aromatic carbons. Upper bounds for distance restraints were classified into ranges of 3.0, 4.0, and 5.5 Å that were based upon relative NOE volumes of the cross peaks. Upper bounds of 4.5 Å were used for distances derived from H^N–H^N NOEs. All lower bounds were set to 1.8 Å. $^3J(H^N,H_\alpha)$ coupling constants were measured from a quantitative HNCA-*J* experiment.[35] The dihedral angle restraints for φ were set to $-120\pm20°$ and $-50\pm20°$ for $^3J(H^N,H_\alpha)$ coupling constants above 8 Hz and below 4 Hz, respectively.

Residual dipolar couplings were measured in aligning medium (5% (C12E5/water) polyoxyethylene-5-lauryl ether (Sigma)/hexan-1-ol (Sigma; $r=0.96$, C12E5/hexan-1-ol) in 20 mM KPO_4, pH 6.2, 50 mM KCl, 10% ^2H_2O).[36] The ^1D(N,H), ^1D(N,C′), and $^2D(H^N,C')$ residual dipolar couplings were extracted from an IPAP-HSQC spectrum;[37] $^1D(C',C_\alpha)$ residual dipolar couplings were extracted from a HNCO-experiment[38,39] without C_α-decoupling; and $^1D(H_\alpha C_\alpha)$ residual dipolar couplings were extracted from a HNCOCA-experiment[40] without H_α-decoupling during carbon evolution. Only peaks that could be tracked reliably and positions that could be determined unambiguously were analyzed. Data for residues with ^1H–^{15}N heteronuclear NOE values less than 0.65 were excluded from the structure calculations.

^{2h}J(N,C′) coupling constants across hydrogen bonds were measured by using a standard 3D HNCO with a 133 ms time for the N–CO transfer step.[41] Hydrogen bond restraints were introduced for each observed ^{2h}J(N,C′) coupling (Figure 1). Hydrogen exchange rates were measured from a series of ^1H,^{15}N-HSQC spectra that were recorded at 25 °C after addition of ^2H_2O to lyophilized protein. The spectra were recorded at 20 min intervals for up to 4 h. Additional hydrogen-bond restraints for amide groups that showed slow exchange were introduced in later stages of structural calculations, when the acceptor group could be identified unambiguously. (Amide groups were still present after 1 h 20 min subsequent to D_2O addition, Figure S1 in the Supporting Information). Every hydrogen-bond restraint was represented by two distance restraints of $2.0\,Å\pm0.3$ (between H and O) and $3.0\,Å\pm0.3$ (between N and O).

Structure calculation: Structures were calculated by using the simulated annealing protocol with torsion-angle dynamics implemented in the CNX 2002 program (Accelrys, Inc., San Diego, CA, USA). In the first step of the calculations, ~2000 NOEs were incorporated into the torsion-angle dynamics and simulated annealing protocols.[42,43] A family of low-energy structures was obtained from these calculations that defined the overall fold. Refinement of these initial structures was accomplished by using the NOAH protocol.[44] New NOE assignments were accepted by NOAH if they agreed with the manually derived NOEs. After twelve iterations, approximately 1000 additional NOE assignments were derived. In the final round of refinement 92 ^1D(N,H), 90 ^1D(N,C′), 91 $^2D(H^N,C')$, 72 $^1D(H_\alpha,C_\alpha)$, 91 $^2D(H^N,C')$, and 84 $^1D(C',C_\alpha)$ residual dipolar couplings were incorporated. NOE-derived distance restraints, angular restraints from TALOS,[45] $^3J(H^N,H_\alpha)$ coupling constants, and hydrogen bond restraints were also incorporated. ^1D(N,C′), $^2D(H^N,C')$, $^1D(C',C_\alpha)$, and $^1D(H_\alpha,C_\alpha)$ values were normalized relative to ^1D(N,H) values.[46] The axial (D_a) and rhombic (D_r) components of the alignment tensor were estimated from the powder pattern of the residual dipolar-coupling histogram and confirmed with the program MODULE.[47,48] The final values of D_a and D_r were approximately 12.4 and 0.24 Hz, respectively. A single alignment tensor was derived for the whole protein. A pseudotetra atom representing the origin of the alignment tensor was introduced for structural calculations by using residual dipolar couplings. The bond length of the pseudoatoms was set to 10 Å to decrease the overall energy and to increase the convergence rate, as described by Ye et al.[49]

Dynamics calculation: ^{15}N-R_1- and ^{15}N-R_2-relaxation rates and $^1H\{^{15}N\}$-HetNOEs were measured as described by Wagner and coworkers.[50] Through the analysis of these spectra, the relaxation histograms that correlated HetNOE values and R_2/R_1 ratios as a function of residue number were calculated. The overall correlation time τ_C was determined from the experimental relaxation data R_2/R_1 by using the Tensor 2.0 program.[30]

Acknowledgements

This work was supported by the Deutsche Forschungsgemeinschaft through the SFB 579 "RNA-Ligand Interactions", the European Large Scale Facility for Biomolecular NMR in Frankfurt (HPRI-1999-CT-00014) and the RTD project FIND STRUCTURE (HPRI-1999-CT-40005).

Keywords: dynamics · NMR spectroscopy · protein structures · ribosome · RNA

[1] N. Leulliot, G. Varani, *Biochemistry* **2001**, *40*, 7947–7956.
[2] M. R. Conte, T. Grune, J. Ghuman, G. Kelly, A. Ladas, S. Matthews, S. Curry, *EMBO J.* **2000**, *19*, 3132–3141.
[3] S. M. Crowder, R. Kanaar, D. C. Rio, T. Alber, *Proc. Natl. Acad. Sci. USA* **1999**, *96*, 4892–4897.
[4] F. H. Allain, D. E. Gilbert, P. Bouvet, J. Feigon, *J. Mol. Biol.* **2000**, *303*, 227–241.
[5] R. C. Deo, J. B. Bonanno, N. Sonenberg, S. K. Burley, *Cell* **1999**, *98*, 835–845.
[6] J. Thompson, E. Cundliffe, M. Stark, *Eur. J. Biochem.* **1979**, *98*, 261–265.
[7] F. J. Schmidt, J. Thompson, K. Lee, J. Dijk, E. Cundliffe, *J. Biol. Chem.* **1981**, *256*, 12301–12305.
[8] M. J. Stark, E. Cundliffe, *J. Mol. Biol.* **1979**, *134*, 767–769.
[9] W. P. Tate, M. J. Dognin, M. Noah, M. Stöffler-Meilicke, G. Stöffler, *J. Biol. Chem.* **1984**, *259*, 7317–7324.
[10] S. Pestka, *Biochem. Biophys. Res. Commun.* **1970**, *40*, 667–674.
[11] E. Cundliffe, P. D. Dixon, *Antimicrob. Agents Chemother.* **1975**, *8*, 1–4.
[12] J. Thompson, E. Cundliffe, M. Stark, *Eur. J. Biochem.* **1979**, *98*, 261–265.
[13] Y. Xing, D. E. Draper, *Biochemistry* **1996**, *35*, 1581–1588.
[14] B. T. Wimberly, R. Guymon, J. P. McCutcheon, S. W. White, V. Ramakrishnan, *Cell* **1999**, *97*, 491–502.
[15] G. L. Conn, D. E. Draper, E. E. Lattman, A. G. Gittis, *Science* **1999**, *284*, 1171–1174.
[16] A. P. Hinck, M. A. Markus, S. Huang, S. Grzesiek, I. Kustonovich, D. E. Draper, D. A. Torchia, *J. Mol. Biol.* **1997**, *274*, 101–113.
[17] M. A. Markus, A. P. Hinck, S. Huang, D. E. Draper, D. A. Torchia, *Nat. Struct. Biol.* **1997**, *4*, 70–77.
[18] Y. Xing, D. Guha Thakurta, D. E. Draper, *Nat. Struct. Biol.* **1997**, *4*, 24–27.

[19] J. Harms, F. Schluenzen, R. Zarivach, A. Bashan, S. Gat, I. Agmon, H. Bartels, F. Franceschi, A. Yonath, *Cell* **2001**, *107*, 679 – 688.
[20] N. Ban, P. Nissen, J. Hansen, P. B. Moore, T. A. Steitz, *Science* **2000**, *289*, 878 – 879.
[21] M. Valle, A. Zavialov, W. Li, S. M. Stagg, J. Sengupta, R. C. Nielsen, P. Nissen, S. C. Harvey, M. Ehrenberg, J. Frank, *Nat. Struct. Biol.* **2003**, *10*, 899 – 906.
[22] R. K. Agrawal, J. Linde, J. Sengupta, K. H. Nierhaus, J. Frank, *J. Mol. Biol.* **2001**, *311*, 777 – 787.
[23] B. T. Porse, I. Leviev, A. S. Mankin, R. A. Garrett, *J. Mol. Biol.* **1998**, *276*, 391 – 404.
[24] M. V. Rodnina, A. Savelsbergh, N. B. Matassova, V. I. Katunin, Y. P. Semenkov, W. Wintermeyer, *Proc. Natl. Acad. Sci. USA* **1999**, *96*, 9586 – 9590.
[25] N. Van Dyke, E. J. Murgola, *J. Mol. Biol.* **2003**, *330*, 9 – 13.
[26] N. Brot, W. P. Tate, C. T. Caskey, H. Weissbach, *Proc. Natl. Acad. Sci. USA* **1974**, *71*, 89 – 92.
[27] S. Ilin, A. Hoskins, H. Schwalbe, J. Wöhnert, *J. Biomol. NMR* **2003**, *25*, 163 – 164.
[28] J. Badger, A. J. Kumar, P. Yip, S. Szalma, *Proteins Struct. Funct. Genet.* **1999**, *35*, 25 – 33.
[29] M. Schubert, D. Labudde, H. Oschkinat, P. Schmieder, *J. Biomol. NMR* **2002**, *24*, 149 – 154.
[30] P. Dosset, J. C. Hus, M. Blackledge, D. Marion, *J. Biomol. NMR* **2000**, *16*, 23 – 28.
[31] B. P. Klaholz, T. Pape, A. V. Zavialov, A. G. Myasnikov, E. V. Orlova, B. Vestergaard, M. Ehrenberg, M. van Heel, *Nature* **2003**, *421*, 90 – 94.
[32] C. Bartels, T. H. Xia, M. Billeter, P. Güntert, K. Wüthrich, *J. Biomol. NMR* **1995**, *5*, 1 – 10.
[33] M. Sattler, J. Schleucher, C. Griesinger, *Prog. Nucl. Magn. Reson. Spectrosc.* **1999**, *34*, 93 – 158.
[34] D. S. Wishart, C. G. Bigam, J. Yao, F. Abildgaard, J. H. Dyson, E. Oldfield, J. L. Markley, B. D. Sykes, *J. Biomol. NMR* **1995**, *6*, 135 – 140.
[35] G. Montelione, G. Wagner, *J. Magn. Reson.* **1990**, *87*, 183 – 188.
[36] M. Rückert, G. Otting, *J. Am. Chem. Soc.* **2000**, *122*, 7793 – 7797.
[37] Y. X. Wang, J. L. Marquardt, P. Wingfield, S. J. Stahl, S. Lee-Huang, D. Torchia, A. Bax, *J. Am. Chem. Soc.* **1998**, *120*, 7385 – 7386.
[38] D. Yang, J. R. Tolman, N. K. Goto, L. E. Kay, *J. Biomol. NMR* **1998**, *12*, 325 – 332.
[39] S. Grzesiek, A. Bax, *J. Magn. Reson.* **1992**, *96*, 432 – 440.
[40] J. R. Tolman, H. M. Al-Hashimi, L. E. Kay, J. H. Prestegard, *J. Am. Chem. Soc.* **2001**, *123*, 1416 – 1424.
[41] F. Cordier, S. Grzesiek, *J. Am. Chem. Soc.* **1999**, *121*, 1601 – 1602.
[42] E. G. Stein, L. M. Rice, A. T. Brünger, *J. Magn. Reson.* **1997**, *124*, 154 – 164.
[43] M. Nilges, A. M. Gronenborn, A. T. Brünger, G. M. Clore, *Protein Eng.* **1988**, *2*, 27-38.
[44] C. Mumenthaler, P. Güntert, W. Braun, K. Wüthrich, *J. Biomol. NMR* **1997**, *10*, 351-362.
[45] G. Cornilescu, F. Delaglio, A. Bax, *J. Biomol. NMR* **1999**, *13*, 289 – 302.
[46] A. Bax, G. Kontaxis, N. Tjandra, *Methods Enzymol.* **2001**, *339*, 127 – 174.
[47] G. M. Clore, A. M. Gronenborn, A. Bax, *J. Magn. Reson.* **1998**, *133*, 216 – 221.
[48] P. Dosset, J. C. Hus, D. Marion, M. Blackledge, *J. Biomol. NMR* **2001**, *20*, 223-231.
[49] K. Ye, A. Serganov, W. Hu, M. Garber, D. J. Patel, *Eur. J. Biochem.* **2002**, *269*, 5182-5191.
[50] K. T. Dayie, G. Wagner, *J. Magn. Reson. Ser. A* **1994**, *111*, 121 – 126.
[51] R. A. Laskowski, D. S. Moss, J. M. Thornton, *J. Mol. Biol.* **1993**, *231*, 1049 – 1067.

Received: March 8, 2005
Published online on August 11, 2005

